Research Square

Preprints are preliminary reports that have not undergone peer review.
They should not be considered conclusive, used to inform clinical practice,
or referenced by the media as validated information.

Drought and salinity recruit largely distinct lncRNAs in sunflower, converging on a compact dual-responsive core

Deniz Sarel
Ankara University
Aybüke Okay
Ankara University
Nilgün Yerli
Ankara University
E. Sümer Aras
Ankara University
İlker Büyük
buyuki@ankara.edu.tr

Ankara University

Research Article

Keywords: Helianthus annuus, long non-coding RNA, competing endogenous RNA, drought, salinity, cross-stress taxonomy, qRT-PCR

Posted Date: September 1st, 2026

DOI: https://doi.org/10.21203/rs.3.rs-10709858/v1

License: This work is licensed under a Creative Commons Attribution 4.0 International License.
Read Full License

Additional Declarations: No competing interests reported.

Abstract

Background

— Drought and salinity increasingly co-occur where sunflower (*Helianthus annuus* L.) is grown, yet which responses the two stresses share and which they keep stress-specific is unknown. Part of that decision is made in the long non-coding RNA (lncRNA) layer, where transcripts carrying microRNA (miRNA)-complementary sites can act as competing endogenous RNAs (ceRNAs) and couple several genes into one module. Sunflower has no abiotic-stress lncRNA catalogue; its stress biology has been resolved only at the coding and small-RNA tiers. We asked whether drought and salinity recruit a shared, dual-responsive lncRNA module, and whether the messenger RNAs (mRNAs) predicted to partner it behave differently in cultivars of contrasting tolerance.

Results

— A three-tool, plant-aware coding-potential consensus with Rfam screening defined 5,046 structurally validated lncRNAs, of which 2,172 were reliably expressed. Testing each stress separately against its own control gave 289 differentially expressed lncRNAs: 196 salinity-specific, 33 drought-specific and only 60 dual-responsive; shared regulation is a compact exception, not a broad common programme. A predicted ceRNA network of 2,575 lncRNA-mRNA edges, built from microRNA target-site prediction and co-expression-module membership, had an mRNA layer over-represented for jasmonate signalling, a candidate stress-responsive axis, and for water-channel activity, a candidate shared osmotic core. Photosynthetic and gravimetric phenotyping confirmed measurable stress responses in both cultivars, the tolerant cultivar cooling its leaves under drought. Quantitative reverse-transcription PCR on the same plants showed the partner mRNAs to be stress-responsive in a genotype- and stress-dependent pattern: under salinity the tolerant cultivar induced sucrose synthase SUS4, while under drought strong induction of the same partners was observed in the sensitive cultivar.

Conclusions

— Sunflower's non-coding stress response resolves into a compact dual-responsive core set against much larger stress-specific fractions, with a candidate jasmonate axis and a candidate shared osmotic core at the drought-salinity intersection. This is the first abiotic-stress-responsive lncRNA and predicted ceRNA framework for the crop and supplies ranked dual-responsive candidates for resilience breeding. Network edges remain sequence-based predictions, and expression-level measurement does not demonstrate microRNA sponging.

Background

Water deficit and soil salinity rarely act in isolation [3]: in the rain-fed and marginally irrigated lands that produce much of the world's oilseed, drought and irrigation-borne salt accumulate in the same fields, so crops face both [4]. The two share an osmotic core yet diverge in their ionic and signalling consequences, and adaptation to one confers only partial cross-resistance [5]. Sunflower (*Helianthus annuus* L.) is grown widely under these conditions. It is the fourth-largest oilseed crop, supplying about 12% of global edible oil [6, 7], and its yield and quality are curtailed by abiotic stress [8]. Agronomic work confirms that salinity, not water deficit alone, sets the realistic ceiling on its yield and germplasm ranking [9, 10]. The question is therefore not how sunflower tolerates drought, but which responses are shared with salinity and which are kept stress-specific.

That decision is made in a layer coding-gene surveys leave invisible. Long non-coding RNAs (lncRNAs), transcripts over 200 nucleotides with little or no coding capacity, act in *cis* and *trans* to tune chromatin state, transcription and RNA stability [11, 12]. One mode suits a shared-response question well: carrying miRNA-complementary sites, lncRNAs can act as target mimics or competing endogenous RNAs (ceRNAs) that sequester a miRNA and relieve its targets from repression [13, 14], coupling several genes into one module. In plants the logic is experimentally grounded, from IPS1's decoy suppression of miR399 [13] to the miR858–phenylpropanoid circuit [15]. A dual-responsive lncRNA can couple genes that both stresses require; a stress-specific one regulates a branch used by only one. That distinction is best exposed at network level.

Across crops, lncRNA–ceRNA modules repeatedly set the gain of drought and salt tolerance, and the best-characterized are cross-stress integrators. The landmark case is *Arabidopsis* DRIR, a lncRNA induced by both drought and salt that positively regulates a shared abscisic acid (ABA)-linked response [16]. Recognised module types include miRNA-decoy ceRNAs [17], crop-scale drought ceRNA catalogues [18, 19] and *cis*/*trans*-acting inventories [20, 21, 22, 23], with mechanisms consolidated in reviews [24, 25, 26]. Almost all of it interrogates a single stress, or stress versus recovery, so a drought-specific/salt-specific/dual-responsive taxonomy has not been drawn even in the best-studied models; and where contrasting genotypes have been compared [27], the modules recovered tracked tolerance, so this layer carries genotype-level, not generic, stress information. These motivate a testable question: do drought and salinity recruit a shared, dual-responsive lncRNA–ceRNA module, and does the behaviour of that module differ between a tolerant and a sensitive genotype?

For sunflower this question is both unasked and answerable. The crop has a chromosome-scale reference genome [28] and its abiotic-stress biology has been dissected only at the coding and small-RNA layers: drought- and salinity-responsive coding genes were reported as early as 2003 [29], drought-responsive miRNAs profiled [30], and tolerant-versus-sensitive contrasts resolved at the coding-gene level by co-expression [31]. Every sunflower lncRNA study to date is instead developmental, biotic or computational: meiocyte [32], endosperm [33] and high-oleic-seed transcriptomes [34], *Sclerotinia*-responsive loci [35] and catalogues [36]. No abiotic-stress lncRNA survey, ceRNA network, drought-versus-salt taxonomy or tolerant-versus-sensitive lncRNA comparison exists for sunflower: the layer most likely to reconcile drought and salinity responses has never been examined.

The study therefore has two layers: deep discovery, then locally relevant expression analysis in characterized plants. From public poly-A transcriptome data of a single genetic background we identify lncRNAs by a plant-trained coding-potential consensus and partition them into drought-specific, salt-specific and dual-responsive classes; co-expression modules and a target-mimicry ceRNA network overlaid on this taxonomy ask where the two programmes converge. Because these edges derive from sequence-based target prediction, they are candidate regulatory hypotheses rather than demonstrated sponge interactions. The network nevertheless holds together, in the associative way that befits a correlative model, around jasmonate-ZIM-domain (JAZ) signalling and water/ion-homeostasis effectors, including aquaporin/water-channel activity and an ABA-linked type-2C protein phosphatase (PP2C), pointing to a candidate shared module at the drought–salt intersection. Because discovery rests on one genotype, the second layer assays these lncRNAs and their predicted mRNA partners by quantitative reverse-transcription PCR (qRT-PCR) in a drought-tolerant and a drought-sensitive cultivar under each stress: a targeted expression-level test, not a transcriptome-wide cultivar comparison. Photosynthetic phenotyping of the same cohort characterizes that material and grounds the cultivar labels in measurement. The work is intended to supply sunflower's first abiotic-stress-responsive lncRNA–ceRNA framework and a set of dual-responsive candidates for breeding stress-resilient oilseed.

Methods

Plant material and stress treatments

Two *Helianthus annuus* L. cultivars, cv. SUN 2235 (drought-tolerant) and cv. Turay (drought-sensitive), were obtained from the Aegean Agricultural Research Institute (İzmir, Türkiye) [37, 38]. Drought was imposed in weight-adjusted soil pots [39, 40]: water was withheld from drought (DR) plants and controls (CK) were irrigated normally. Dry-down was monitored gravimetrically every two days; by day 7 after final irrigation droughted pots had lost 72.8% (SUN 2235) and 73.1% (Turay) of their initial weight while control pots gained 8.8% and 10.7% (Fig. 6C), so drought severity was equivalent between genotypes. Salinity was imposed hydroponically: at the three-leaf stage plants were split into CK and salinity (SA; +150 mM NaCl) groups for 7 days. Leaf and root were collected in three biological replicates, matching the *in silico* discovery design and avoiding a tissue-mismatch confound (growth-chamber and treatment details in Additional file 1). The drought (soil) and salinity (hydroponic) cohorts are separate experiments, each with its own matched control against which qRT-PCR is read; the drought-versus-salinity contrast rests on the single-study *in silico* dataset, supported by qRT-PCR one stress at a time.

Photosynthetic phenotyping

Before harvest, the whole treated cohort, from which the three biological replicates used for RNA extraction were subsequently drawn, was phenotyped with a MultispeQ v2 fluorometer (PhotosynQ) under ambient light, recording photosystem II quantum yield (Φ_II), the regulated (Φ_NPQ) and non-regulated (Φ_NO) dissipation yields, NPQ(T), qL, Fv'/Fm', linear electron flow (LEF), relative chlorophyll

(SPAD) and leaf temperature. Three leaves per plant were averaged, making the plant the unit of analysis: drought, SUN 2235 n = 5 control / 9 stress and Turay n = 5 / 10; salinity, n = 7 per group. Stress and matched control were compared within cultivar by Welch's unequal-variance t-test with Benjamini–Hochberg correction across all 36 tests ($q < 0.05$ significant). No cultivar × treatment interaction model was fitted, so between-cultivar statements are descriptive comparisons of within-cultivar responses. Measurements are single-time-point, light-adapted fluorescence parameters: gas exchange, water potential and tissue ion content were not measured, so leaf-temperature differences are read only as consistent with differing transpiration. Measurements were made under ambient rather than fixed light, so linear electron flow (LEF), which the MultispeQ computes as Φ_II × incident photosynthetically active radiation, depends on the light environment in a way the dimensionless yields do not.

RNA-seq data and read processing

lncRNA discovery used the strand-specific multi-stress dataset of Barnhart et al. [1] (PRJNA742396), restricted to its CK, DR (dry-down) and SA (NaCl) arms: 23 paired-end, poly-A-selected libraries. Because poly-A selection under-samples non-polyadenylated transcripts, the catalogue is expected to be enriched for polyadenylated lincRNA/antisense/intronic lncRNAs (Discussion). Reads were trimmed with fastp [41] and aligned to HanXRQr2.0-SUNRISE (Ensembl Plants release 62; [28]) with HISAT2 [42] in reverse-stranded mode, confirmed empirically with RSeQC [43], then assembled, merged and quantified with StringTie [44]. Versions and parameters are in Additional file 1.

lncRNA identification and the two-tier catalogue

Strict criteria guarded against mis-classifying mRNA isoforms as lncRNAs: gffcompare [45] class codes restricted to intergenic, intronic, antisense and other-overlap transcripts (u/i/x/o); FEELnc_filter [46] removal of transcripts < 200 nt and of sense overlaps with protein-coding exons; a three-tool, plant-aware coding-potential consensus requiring unanimous non-coding calls from PlantLncBoost [47], CPC2 [48] and Pfam-A/HMMER [49, 50]; and Rfam/Infernal removal of housekeeping ncRNAs [51, 52] (per-step counts in Fig. 1a,b and Additional file 2: Table S1; tool versions and parameters in Additional file 1). Because FEELnc_filter removes single-exon transcripts, the catalogue is inherently multi-exonic, so the mono-exonic assembly- or transposon-artefact concern does not arise.

Transcripts reaching a transcripts-per-million (TPM) value ≥ 0.5 in at least two biological replicates of at least one stress × tissue group formed the expressed tier, giving a two-tier catalogue of 5,046 structurally validated lncRNAs (genomic context assigned with FEELnc_classifier) and 2,172 expressed lncRNAs (Fig. 1c); all downstream analysis uses the expressed tier. lncRNA exons proved *less* repeat-rich than length-matched random intervals (Fig. 1d), so no repeat-based exclusion was applied.

Differential expression and cross-stress classification

Because tissue dominated the primary axis of variation in principal component analysis (PCA; PC1 = 82%), DESeq2 [53] was run per tissue rather than with a tissue covariate, testing DR versus CK and SA versus CK; $|\log_2 FC| \geq 1$ with Benjamini–Hochberg (BH)-adjusted $p < 0.05$ defined differentially expressed lncRNAs (DELs) and genes (DEGs). Two PCA-outlier libraries were removed, leaving 21 (leaf $n = 10$, root $n = 11$). Cultivar comparison was reserved for qRT-PCR, as PRJNA742396 includes neither cultivar. Four of the six groups had three biological replicates, and replication was unequal between the salt (4–5) and drought (3) arms. DELs were partitioned across the two separately tested stresses into drought-specific, salinity-specific and dual-responsive (differentially expressed under both, each against its own control) classes, and resolved by tissue (Fig. 2).

Co-expression network analysis

Separate signed leaf and root networks were built by weighted gene co-expression network analysis (WGCNA; [54]) from variance-stabilized counts of expressed mRNAs and lncRNAs, at powers giving approximately scale-free topology. Module eigengenes were correlated with stress condition, and non-grey hub lncRNAs of stress-associated modules became qRT-PCR candidates (thresholds in Additional file 1).

Cis- and trans-target prediction

Cis-targets were protein-coding genes within ± 100 kb of a DEL correlating with it at Spearman $|\rho| \geq 0.8$ and BH-FDR < 0.05 in at least one tissue (sensitivity to the correlation cutoff in Additional file 1). Trans-targets were protein-coding genes in the same non-grey WGCNA module as a DEL. Because strong cis co-expression is rare (proximity does not imply co-regulation), trans/same-module is the primary evidence and cis supporting.

ceRNA network construction

A set of 892 mature miRNAs (miRBase; *H. annuus* han- entries where available, otherwise ath- and gma-families) was screened with psRNATarget [55] against the 289 DEL lncRNAs and 694 module-associated DEG mRNAs (Expectation ≤ 5 both sides; sensitivity to a stricter cutoff in Additional file 1). A predicted competing endogenous RNA relationship was a lncRNA–mRNA pair bridged by ≥ 1 shared miRNA *and* co-occurring in the same non-grey tissue WGCNA module (distinct loci); networks were assembled in Cytoscape [56]. Because this rule merely adds a shared-miRNA requirement to the same-module rule, ceRNA edges are a strict subset of the trans pairs; their overlap is a pipeline-consistency check, not independent convergent evidence. For legibility, Fig. 4a retains edges with ≥ 3 shared miRNAs or involving a qRT-PCR panel lncRNA; this rule governs the display only and not the analysis.

Functional annotation and enrichment

Annotation used eggNOG-mapper v2 against eggNOG v5 (Viridiplantae; [57, 58]). Gene Ontology (GO; biological process, molecular function, cellular component), KEGG orthologue and KEGG pathway over-representation were tested hypergeometrically (BH FDR < 0.05) on the expressed-tier ceRNA-network mRNAs (540 genes, 521 annotated) against the annotated DEG background (6,900 genes); reporting filters and quality-control exclusions are in Additional file 1.

qRT-PCR expression analysis

Total RNA was extracted, DNase I-treated and reverse-transcribed, and gene-specific primers were designed and specificity-screened for selected network-stage lncRNAs and their predicted ceRNA-partner mRNAs (18 primer pairs); primer sequences are given in Additional file 2: Table S2 and assay-level quality-control information in Additional file 1. Amplification used SYBR Green chemistry on a Bio-Rad CFX96 real-time system following Büyük et al. [2], with reagents, cycling and replicate handling in Additional file 1. The panel was measured across the stress × cultivar × tissue groups of the design, and relative expression was calculated by the 2^−ΔΔCT method [60] after normalization to the geometric mean of ACTIN (ACT) and elongation factor 1-α (EF-1α) (MIQE; [59]). Groups with insufficient biological replication, or failing the detection, specificity or reference-gene criteria, were excluded from quantitative interpretation and are identified in Additional file 1. Amplification efficiencies were not determined empirically and no − RT controls were included; these limitations are carried into the interpretation of the qRT-PCR data.

Statistical analysis and visualization

Given the cohort's supporting role and limited replication, qRT-PCR results are reported descriptively as fold change and direction relative to each stress control (ΔΔCT in Additional file 1). Welch's unequal-variance *t*-tests are exploratory; per-contrast *p*-values are quoted uncorrected, with a Benjamini–Hochberg correction across the computable partner-mRNA contrasts reported alongside in the Results. No interaction or between-cultivar test was performed.

Results

A conservatively filtered, two-tier lncRNA catalogue

A genome-guided assembly filtered through a plant-aware cascade reduced 219,988 assembled transcripts to 6,250 candidates (Fig. 1a; per-step counts in Additional file 2: Table S1). Unanimous non-coding calls from PlantLncBoost (5,409), CPC2 (5,455) and a Pfam-negative screen (5,245) converged on 5,048 high-confidence lncRNAs (Fig. 1b); Rfam/Infernal screening removed 2 housekeeping rRNA transcripts (SSU, LSU), leaving 5,046, and an expression floor (TPM ≥ 0.5 in ≥ 2 biological replicates of ≥ 1 stress×tissue group) defined the 2,172-lncRNA expressed tier (Fig. 1c).

Catalogue features were typical of plant lncRNAs (Figure S1a–d): median length 345 nt; 86% two-exon loci, none mono-exonic by FEELnc_filter design; an even spread across the 17 assembled chromosomes; predominantly intergenic FEELnc classification. lncRNA exons averaged 68.1% repeat-masked content,

intermediate between protein-coding exons (27.3%) and length-matched random genomic intervals (83.2%) (Fig. 1d); below the random-genome baseline, they showed no transposon enrichment, and no repeat-based exclusion was applied.

Salinity mobilizes a broader lncRNA repertoire than drought

Tissue explained 82% of variance on PC1, so DESeq2 was run per tissue ($|\log_2 FC| \geq 1$, padj < 0.05) for the drought- and salt-versus-control contrasts. The two stresses were analysed separately, so "dual-responsive" strictly denotes a locus significant in both single-stress contrasts rather than any combined-stress condition; both contrasts draw on the same control libraries, which correlates them and can inflate the dual-responsive class, and the two stresses were not formally compared. DEL counts were markedly asymmetric (Fig. 2a): leaf-drought 15, leaf-salt 76, root-drought 81, root-salt 192; the same scaling held transcriptome-wide (root-salt 2,952 down, 5,435 up; Fig. 2c).

The union gave 93 drought-responsive and 256 salt-responsive DELs, 289 unique, partitioned into 33 drought-specific (11%), 196 salt-specific (68%) and 60 dual-responsive (21%) loci (Fig. 2b,d), a substantially broader, largely non-overlapping salt repertoire. The network and enrichment analyses below are built on all 289 DELs, not on the dual-responsive subset alone.

Distinct co-expression modules track salinity and drought

Per-tissue signed WGCNA networks supplied co-membership evidence (soft-thresholding powers and module counts in Fig. 3). Module eigengene–trait correlation ($|r| > 0.5$, $p < 0.05$, uncorrected; this screen selects candidates and is not itself a result) recovered distinct modules tracking salt versus drought in each tissue (Fig. 3): in leaf, turquoise ($r = 0.96$) tracked salt positively and green ($r = -0.94$) negatively ($p < 0.001$), while lightcyan tracked drought ($r = 0.87$, $p < 0.01$); in root, turquoise ($r = 0.97$) tracked salt positively and blue ($r = -0.98$) negatively ($p < 0.001$), while brown ($r = 0.83$) and pink ($r = 0.80$) tracked drought ($p < 0.01$). Of 361 hub lncRNAs (kME > 0.8; 144 leaf, 217 root), 164 were also DELs; these doubly-evidenced loci were prioritized as qRT-PCR candidates.

A DEL-anchored, predicted ceRNA network

A DEL-anchored competing-endogenous-RNA (ceRNA) network was built, every edge a sequence-prediction hypothesis, not a demonstrated sponge interaction: 892 miRBase miRNAs (han-/ath-/gma-) were screened with psRNATarget against the 289 DEL lncRNAs and 694 module-associated DEG mRNAs, an edge requiring ≥ 1 shared miRNA plus co-membership in the same non-grey WGCNA module. On the expressed tier it comprised 2,575 lncRNA–mRNA edges among 1,041 nodes (540 mRNAs, 390 miRNAs and only 111 of the 289 DEL lncRNAs) and 3,278 lncRNA–miRNA–mRNA triplets (Fig. 4). Shared-miRNA support per edge had median 1, maximum 19 (1:2,073; 2:386; 3:88; 4:15; 5:5; 6–19:8), so the bulk of predicted edges are single-miRNA hypotheses.

A core sub-network of edges with ≥ 3 shared miRNAs or a qRT-PCR-panel lncRNA comprised 254 edges among 44 lncRNAs and 176 mRNAs (Fig. 4a); nine of the 10 network-stage candidate lncRNAs appeared, the absent locus having no co-expressed partner. The panel's only dual-responsive locus, MSTRG.59498.1, was predicted to share 4 miRNAs (ath-miR4243, ath-miR837-5p, ath-miR866-5p, gma-miR1512a-3p) with 22 mRNAs across 23 triplets (Fig. 4b). Four panel lncRNAs had functionally suggestive predicted partners (MSTRG.59498.1→SAMT/JMT, a salicylate/jasmonate carboxyl methyltransferase; MSTRG.75989.1→PIP aquaporin; MSTRG.39913.1→LOX2S; and MSTRG.55643.2→PP2C), but each rests on a single shared miRNA, the weakest evidence tier, and is presented only as a candidate for experimental follow-up.

The network converges on jasmonate signalling and water/ion homeostasis

Of the 540 ceRNA-network mRNAs, 521 annotated (eggNOG-mapper v2) were tested by hypergeometric enrichment (BH-FDR < 0.05) against 6,900 annotated DEGs. Of 134 significant GO terms, 115 were reportable after excluding 19 obsolete in the current release, along with 15 reportable KEGG orthologs (KO) and 7 reportable KEGG pathways; non-plant cross-maps and umbrella pathways were excluded on the same basis. Two themes dominated (Fig. 5).

The first was jasmonate signalling and biosynthesis: regulation of jasmonic acid–mediated signalling (GO:2000022) was enriched 7.1-fold and the jasmonate-ZIM-domain (JAZ) repressor ortholog K13464 ranked among the most strongly enriched targets (FDR ≈ 1×10^{-8}), with upstream and biosynthetic signatures including α-linolenic acid metabolism (map00592) and lipoxygenase (LOX). Transcription corepressor activity (GO:0003714, 10.0-fold) belongs to this theme and is not a separate signal, JAZ proteins being themselves corepressors.

The second was water and ion homeostasis, enriched for water channel activity (GO:0015250, 4.4-fold, FDR 4.3×10^{-4}), response to water deprivation (GO:0009414, 2.3-fold), monoatomic ion transport (GO:0006811), the ABA-linked PP2C (K14497) and plant hormone signal transduction (map04075). The enriched aquaporin ortholog was the tonoplast intrinsic protein TIP (K09873); the plasma-membrane PIP class (K09872) was not significant and is not reported as enriched.

Because this enrichment covers the entire 540-mRNA layer (including salt-specific- and drought-specific-anchored nodes, not only the dual-responsive core), it characterizes that layer as a whole rather than demonstrating that the intersection loci drive these themes. A network built without reference to functional annotation was nonetheless enriched for two stress-relevant themes: jasmonate signalling, a candidate stress-responsive axis, and aquaporin/water-channel with ion homeostasis, a candidate shared osmotic core at the drought–salinity intersection.

Cis and trans target relationships

The trans rule (same non-grey WGCNA module as a DEL) yielded 52,786 lncRNA–mRNA pairs across 1,259 genes, the primary co-expression evidence. The cis rule (within ± 100 kb, $|\rho| \geq 0.8$, BH-FDR < 0.05)

yielded only 4 cis-target pairs (leaf 3, root 2, 1 shared); relaxing the correlation cutoff added none (Additional file 1). The standout cis pair, the salt-responsive lncRNA MSTRG.3487.1 with HanXRQr2_Chr01g0021851 506 bp away, was significant in both tissues (ρ_leaf 0.997, FDR 2.9×10^{-8}; ρ_root 0.901, FDR 0.013), arguing against a tissue-composition artefact.

Physiological verification of the stress treatments and the cultivar contrast

Photosynthetic phenotyping of the cohort from which the RNA-sampled plants were drawn (n = 5–10 per drought group, 7 per salinity group) confirmed a measurable stress response in both cultivars under both stresses, 26 of 36 tests surviving Benjamini–Hochberg correction. Φ_II fell in all four cultivar–stress groups (− 1.39% to − 2.59%; q ≤ 0.0156) and qL with it (− 2.59% to − 4.66%; q ≤ 0.0463), while Φ_NPQ rose in all four (+ 17.52% to + 33.67%; q ≤ 0.0473), NPQ(T) tracking it in three, the canonical photoprotective signature (Fig. 6A,B). Gravimetric dry-down verified the treatment: droughted pots lost 72.8% (SUN 2235) and 73.1% (Turay) of initial weight by day 7 while controls gained weight; the cultivars dried at indistinguishable rates, so the genotype differences below are not explained by unequal drought severity (Fig. 6C).

Under drought Turay showed the larger photoprotective response (Φ_NPQ + 25.98%, q = 0.0009; NPQ(T) + 24.12%, q = 0.0012) and lost 11.94% of LEF (q = 0.0111), which SUN 2235 maintained (not significant; Fig. 6A); SUN 2235 also cooled its leaves by 1.66°C (27.55 versus 29.21°C; q = 0.0331; not plotted), consistent with sustained transpiration, unlike Turay. Under salinity SUN 2235 mounted the stronger regulated response (Φ_NPQ + 33.67%, q = 0.0006; NPQ(T) + 30.51%, q = 0.0012) while increasing LEF (+ 9.19%, q = 0.0061), whereas Turay's NPQ(T) and LEF responses did not survive correction (Fig. 6B). The LEF contrasts are reported as provisional, because LEF scales with the incident light at measurement (Methods). Magnitudes are moderate and no cultivar × treatment interaction was fitted, so between-cultivar statements are descriptive contrasts characterizing the sampled plants; they do not test the predicted network or its candidate axes.

Expression analysis of selected ceRNA-associated transcripts by qRT-PCR

qRT-PCR showed stress-responsive expression among the network's predicted ceRNA-partner mRNAs in both cultivars (Fig. 7). Of the 34 computable partner-mRNA contrasts, 12 reached $p < 0.05$ and 7 survived Benjamini–Hochberg correction at $q < 0.05$, so only the largest effects are secure. The tally is descriptive, but it shows on an independent platform that the network's mRNA layer contains stress-regulated genes (Fig. 7C). Five partner mRNAs, together with their lncRNA partners (Additional file 1), were assayed in drought-tolerant SUN 2235 and drought-sensitive Turay in a 2 stress × 2 cultivar × 2 tissue × 2 condition design, each stress against its own control; each lncRNA has several predicted partners, and the assayed partner is not in every case the one highlighted in the enrichment analysis above.

Salinity, the stress the panel was designed around, separated the two cultivars in part of the panel (Fig. 7A,B). SUS4 rose in SUN 2235 root (+ 2.42 $\log_2$FC, 5.34×, $p = 0.005$) while falling in Turay (leaf 0.30×, root 0.25×); the SUN 2235 leaf value (+ 3.10, 8.55×) rests on a single replicate and is not interpreted quantitatively. HanXRQr2_Chr07g0278911 likewise rose in SUN 2235 root (+ 1.91, 3.76×, $p = 0.032$) while falling in Turay root (0.04×), and the RING-type E3 ligase (RING-E3) showed a large nominal increase in SUN 2235 leaf (54.1×, $p = 0.040$) that did not remain significant after correction. Not every partner followed this pattern: BT1 was consistently repressed under salt in both cultivars (SUN 2235 root 0.48×, $p = 0.004$; Turay leaf 0.11×, $p = 0.024$; Turay root 0.28×, $p = 0.044$), and the amino-acid permease was mixed, induced in Turay root (+ 1.52 $\log_2$FC, 2.87×, $p = 0.006$) and repressed in SUN 2235 leaf (0.37×) (Fig. 7C).

Under drought, strong induction of SUS4 (+ 6.30 $\log_2$FC, $p < 0.001$) and RING-E3 (+ 5.1, $p < 0.001$) was observed in the sensitive cultivar, particularly in leaf tissue, with RING-E3 also induced in root (+ 5.1, $p = 0.003$). The drought contrasts in SUN 2235 did not meet the reference-gene criterion and are not interpreted quantitatively (Methods). The pattern is therefore stress- and genotype-dependent rather than a simple tolerant superiority, which was not formally tested; magnitudes were normalization-sensitive, but the direction of the salinity cultivar contrast held under all three normalization schemes (Additional file 1).

The lncRNA assays did not support quantitative interpretation and are therefore not considered further (assay-level quality control in Additional file 1). The qRT-PCR data consequently provide expression-level support for selected mRNA components of the predicted network rather than functional evidence for ceRNA interactions.

Discussion

Sunflower's drought and salinity responses had been resolved only in the coding and small-RNA tiers, leaving open which are shared and which stress-specific. At the non-coding level the answer is asymmetric: of 289 differentially expressed lncRNAs (DELs), most are stress-specific, and a compact core of 60 (21%) responds in both single-stress contrasts. Weighted co-expression and a predicted competing-endogenous-RNA (ceRNA) network point to two candidate axes at the drought–salinity intersection, jasmonate signalling as a candidate stress-responsive axis and water/ion homeostasis as a candidate shared osmotic core, plus a candidate ABA-linked PP2C node; targeted qRT-PCR in a drought-tolerant and a drought-sensitive cultivar shows genotype- and stress-dependent expression of the network's partner mRNAs. The supporting two-tier catalogue (5,046 structurally validated loci, 2,172 reliably detected) is sunflower's first abiotic-stress lncRNA catalogue, and it provides the substrate for the analyses reported here.

The taxonomy is conspicuously salt- and root-dominant: salinity mobilized roughly 2.75-fold more lncRNAs than drought (256 versus 93 responsive loci), and in every contrast the root recruited more DELs than the leaf. This ratio is a property of the present dataset rather than a fixed constant, since its

magnitude will reflect treatment severity, kinetics, unequal replication (salt arms 4–5 libraries against 3 for drought) and the single discovery genotype. Its direction is expected: salinity adds an ionic load to the osmotic deficit it shares with drought, and the root is the interface for water uptake and Na^+ exclusion, consistent with acclimation to one stress conferring only partial cross-resistance to the other [5]. The salt-specific majority (196 of 289 DELs) tempers expectations of a symmetric shared programme: shared regulation appears to be the exception, not the rule.

The first of the network's two candidate axes is jasmonate signalling. Its mRNA layer is over-represented for regulation of jasmonate-mediated signalling (GO:2000022, 7.1-fold) and recruits both arms of the pathway: biosynthesis (α-linolenic acid metabolism, map00592) and signalling (the jasmonate-ZIM-domain repressor JAZ, K13464; FDR ≈ 1×10^{-8}). Transcription-corepressor activity (GO:0003714, 10.0-fold) belongs to the same theme and is not an incidental signal: JAZ proteins are corepressors. However, this interpretation is limited by two considerations. The enrichment is computed over the whole 540-mRNA layer, so it speaks to that layer's composition and is no evidence that the 60 dual-responsive loci, or any class, drive jasmonate output; and because the layer is anchored on the 111 of 289 DELs entering the network, an input set dominated by the 196 salt-specific loci, a whole-layer signal cannot be partitioned between shared and salt-specific programmes. Jasmonate is therefore a candidate stress-responsive axis, not a demonstrably shared one.

The second candidate axis is water and ion homeostasis. The same layer is over-represented for water-channel activity and response to water deprivation, with the significant aquaporin signal resolving specifically to the tonoplast intrinsic protein (TIP) class, not the plasma-membrane PIP class. Alongside these sit monoatomic ion transport and plant hormone signal transduction, with the enriched ABA-linked PP2C sitting within the PYR/PYL–PP2C–SnRK2 module that tunes the ABA response *Arabidopsis* DRIR first tied to dual drought-and-salt regulation [16]; only the phosphatase is over-represented, so this module is cited as context rather than as an enriched triad. Unlike jasmonate, the sharedness of this axis does not rest on enrichment alone: osmotic adjustment is by definition a response drought and salinity hold in common, so water/ion homeostasis stands as a candidate shared osmotic core. It remains a candidate, not a proven route.

Our 60 dual-responsive loci are the candidate sunflower counterpart to DRIR; comparable modules recur across lineages [17, 18, 23, 25]. Where contrasting-tolerance genotypes have been compared [27], the non-coding layer carried genotype-level rather than generic stress information, which is the premise our cultivar contrast tests; sunflower had been absent from this map.

Recent work in a distant eudicot offers a parallel: in *Cannabis sativa* (Rosales), drought recruited PP2C into the top ceRNA module in a classical up-up sponge configuration (MSTRG.14087–gma-miR1533–PP2C; [61]); sunflower (Asterales) likewise enriches an ABA-linked PP2C (K14497), predicted as a panel lncRNA's partner (MSTRG.55643.2, on a single shared miRNA, the weakest evidence tier). Two cautions apply: both analyses share one predicted-ceRNA pipeline and overlapping cross-species (gma-) miRBase sets, so methodological and annotation bias is a live alternative to biological convergence; and PP2C is

among the most reliably ABA- and drought-induced gene families, so its recovery in two networks is closer to expected than coincidental. With those caveats, that both networks route an ABA-linked PP2C through lncRNA–ceRNA circuits remains suggestive, the more so because the surrounding modules diverge, consistent with a regulatory layer of low primary-sequence conservation but conserved logic [11]. That study also found a predicted sponge edge whose partner moved opposite to expectation: directional concordance is a hypothesis to test, not a property to assume.

Every ceRNA edge is a prediction: a psRNATarget-inferred shared miRNA-binding site plus co-membership of one co-expression module, and therefore a candidate target-mimicry hypothesis [13, 14], not a demonstrated sponge interaction, which only manipulation can confirm [15]. The enrichment characterizes the 540-mRNA layer as a whole, speaking to that layer's composition rather than to causal flow through any locus, and the same caution applies to the strongest cis association, in which a salt-responsive lncRNA (MSTRG.3487.1) lies 506 bp from an uncharacterized protein-coding neighbour and co-varies with it almost perfectly in both tissues ($\rho = 0.997$ and 0.901), since proximity is not co-regulation. The network is therefore best regarded as a ranked set of hypotheses.

The cultivar designations no longer rest on prior literature alone. Photosynthetic phenotyping of the sampled plants shows a measurable, if moderate, photoprotective response to both stresses in both cultivars and a divergence between them: under drought the sensitive Turay mounted the larger photoprotective response while the tolerant SUN 2235 cooled its leaves by 1.66°C, consistent with maintained transpiration; under salinity SUN 2235 mounted the stronger regulated photoprotective response. These are single-time-point light-adapted fluorescence measurements and descriptive cultivar contrasts: they characterize the plants and test neither the predicted network nor its candidate axes.

The qRT-PCR profiles differed across stress and cultivar contexts. Under salinity the tolerant cultivar induced SUS4 and the Chr07g0278911 partner in root, while BT1 was repressed in both cultivars; under drought, strong induction of SUS4 and RING-E3 was observed in the sensitive cultivar, particularly in leaf tissue (Fig. 7). Because the assay measures transcript abundance, these data support the network's mRNA layer at the expression level and not sponge function, and the contrast between cultivars is descriptive.

Several boundaries follow from the design. Discovery rested on poly-A–selected transcriptomes, so the catalogue is enriched for polyadenylated lncRNAs and under-samples non-polyadenylated species; the complement we report is a floor, not a census. The taxonomy was drawn in a single genetic background, so the dual-responsive claim is for now a one-genotype result, and catalogues of this kind remain sensitive to assembly and annotation choices [36]. On the network side the miRNA arm draws on cross-species miRBase entries (han-, ath-, gma-) rather than an in-house small-RNA dataset, cis assignment within ± 100 kb is a proximity proxy, and the evidence is thin per edge: 2,073 of the 2,575 ceRNA edges rest on a single shared miRNA, the weakest tier, including all four panel-lncRNA partners (SAMT/JMT, PIP aquaporin, LOX2S, PP2C). Because the ceRNA rule is nested inside the co-expression rule, those 2,575 edges are a strict subset of the 52,786 same-module pairs, so their agreement is a pipeline-

consistency check rather than independent support. A stricter miRNA-side cutoff returned no interactions at all, so the network is also sensitive to that parameter. Replication in the discovery libraries was unequal between the two stress arms, and experimental support was further limited by unequal qRT-PCR replication and by assay and reference-gene performance in a subset of contrasts.

Conclusions

Sunflower's non-coding stress response thus resolves into a compact dual-responsive core, a candidate stress-responsive jasmonate axis and a candidate shared osmotic core of water/ion homeostasis at the drought–salinity intersection, with a candidate conserved ABA/PP2C node. These are hypotheses, not proven mechanism. For the fourth-largest oilseed crop, grown where drought and salinity increasingly co-occur and curtail yield [4, 6, 8], a ranked inventory of dual-responsive loci is an entry point for resilience breeding, and the larger set of 164 doubly-evidenced loci, differentially expressed *and* network hubs, offers prioritizable markers and, in time, targets for allele mining or editing. Moving from prediction to function means ribo-depleted RNA-seq, in-house small-RNA and degradome sequencing to test predicted edges, perturbation of top candidates anchored to field and physiological phenotyping, and transcriptome-wide extension of the cultivar contrast.

Abbreviations

ABA, abscisic acid; ACT, actin; BH, Benjamini–Hochberg; ceRNA, competing endogenous RNA; CK, control; Cq, quantification cycle; DEG, differentially expressed gene; DEL, differentially expressed lncRNA; DR, drought; EF-1α, elongation factor 1-α; FDR, false discovery rate; Fv'/Fm', maximum efficiency of photosystem II in the light-adapted state; GO, Gene Ontology; JAZ, jasmonate-ZIM-domain; KEGG, Kyoto Encyclopedia of Genes and Genomes; KO, KEGG Orthology; kME, module membership; LEF, linear electron flow; lncRNA, long non-coding RNA; MIQE, Minimum Information for Publication of Quantitative Real-Time PCR Experiments; miRNA, microRNA; mRNA, messenger RNA; NPQ, non-photochemical quenching; PAR, photosynthetically active radiation; PCA, principal component analysis; PIP, plasma-membrane intrinsic protein; PP2C, type-2C protein phosphatase; qL, fraction of open photosystem II centres; qRT-PCR, quantitative reverse-transcription PCR; SA, salinity; SPAD, relative chlorophyll content; TIP, tonoplast intrinsic protein; TPM, transcripts per million; WGCNA, weighted gene co-expression network analysis; Φ_II, quantum yield of photosystem II; Φ_NPQ, quantum yield of regulated non-photochemical dissipation; Φ_NO, quantum yield of non-regulated dissipation.

Declarations

Ethics approval and consent to participate

Not applicable. This study involved no human participants, human data, human tissue or animals. The sunflower cultivars used are commercially available breeding material obtained from the Aegean Agricultural Research Institute (İzmir, Türkiye).

Consent for publication

Not applicable.

Availability of data and materials

The RNA-sequencing data underlying the discovery analyses are publicly available from the NCBI Sequence Read Archive under BioProject accession PRJNA742396 (https://www.ncbi.nlm.nih.gov/bioproject/PRJNA742396). No new sequencing data were generated in this study. The derived datasets analysed during the current study — the two-tier lncRNA catalogue (GTF and FASTA), the differential-expression tables, the co-expression module assignments, the microRNA query set, the target-prediction output and the competing-endogenous-RNA network files — are available from the corresponding author on reasonable request. All other data supporting the findings of this study are included in this published article and its additional file.

Competing interests

The authors declare that they have no competing interests.

Funding

This study was financially supported by the Scientific Research Projects Coordination Unit (BAP) of Ankara University under Project No. FBA-2026-5368 and Project No. FYL-2022-2760. D.S. is supported by the 2211-E National PhD Scholarship Program for Priority Areas from the Scientific and Technological Research Council of Türkiye (TÜBİTAK).

Authors' contributions

DS conceived the study, curated the data, performed the formal analysis, the bioinformatic investigation and the visualization, and wrote the original draft. NY and AO performed the experimental investigation and validation. ESA and İB supervised the study and reviewed and edited the manuscript; İB also conceived the study, administered the project and provided resources. All authors read and approved the final manuscript.

Acknowledgements

Not applicable.

References

1. Barnhart MH, Masalia RR, Mosley LJ, Burke JM. Phenotypic and transcriptomic responses of cultivated sunflower seedlings (Helianthus annuus L.) to four abiotic stresses. PLoS ONE. 2022;17(9):e0275462. 10.1371/journal.pone.0275462.

2. Büyük İ, İlhan E, Şener D, Özsoy AU, Aras S. Genome-wide identification of CAMTA gene family members in Phaseolus vulgaris L. and their expression profiling during salt stress. Mol Biol Rep. 2019;46(3):2721–32. 10.1007/s11033-019-04716-8.
3. Bai Y, Kissoudis C, Yan Z, Visser RGF, van der Linden G. Plant behaviour under combined stress: tomato responses to combined salinity and pathogen stress. Plant J. 2018;93(4):781–93. 10.1111/tpj.13800.
4. Priya P, Patil M, Pandey P, Singh A, Babu VS, Senthil-Kumar M. Stress combinations and their interactions in plants database: a one-stop resource on combined stress responses in plants. Plant J. 2023;116(4):1097–117. 10.1111/tpj.16497.
5. Cao H, Ding R, Du T, Kang S, Tong L, Chen J, et al. A meta-analysis highlights the cross-resistance of plants to drought and salt stresses from physiological, biochemical, and growth levels. Physiol Plant. 2024;176(2):e14282. 10.1111/ppl.14282.
6. Rauf S, Jamil N, Tariq SA, Khan M, Kausar M, Kaya Y. Progress in modification of sunflower oil to expand its industrial value. J Sci Food Agric. 2017;97(7):1997–2006. 10.1002/jsfa.8214.
7. Adeleke BS, Babalola OO. Oilseed crop sunflower (Helianthus annuus) as a source of food: nutritional and health benefits. Food Sci Nutr. 2020;8(9):4666–84. 10.1002/fsn3.1783.
8. Kefale H, You J, Zhang Y, Getahun S, Berhe M, Abbas AA, et al. Metabolomic insights into the multiple stress responses of metabolites in major oilseed crops. Physiol Plant. 2024;176(6):e14596. 10.1111/ppl.14596.
9. Canavar Ö, Gören HK, Tan U, Yilmaz O, Kaptan MA, Küçük Kaya S. Physiological responses of sunflower (Helianthus annuus L.) to multiple combined prolonged drought stress, salinity stress and boron toxicity. J Agron Crop Sci. 2025;211(2):e70047. 10.1111/jac.70047.
10. Saylak S, Irmak S, Eskridge KM, Dweikat I. Sunflower germplasms' response to different water and salinity stress levels in greenhouse and field conditions under subsurface drip irrigation. Irrig Sci. 2025;74(1):161–81. 10.1002/ird.2977.
11. Lucero L, Ferrero L, Fonouni-Farde C, Ariel F. Functional classification of plant long noncoding RNAs: a transcript is known by the company it keeps. New Phytol. 2021;229(3):1251–60. 10.1111/nph.16903.
12. Statello L, Guo CJ, Chen LL, Huarte M. Gene regulation by long non-coding RNAs and its biological functions. Nat Rev Mol Cell Biol. 2021;22(2):96–118. 10.1038/s41580-020-00315-9.
13. Franco-Zorrilla JM, Valli A, Todesco M, Mateos I, Puga MI, Rubio-Somoza I, et al. Target mimicry provides a new mechanism for regulation of microRNA activity. Nat Genet. 2007;39(8):1033–7. 10.1038/ng2079.
14. Salmena L, Poliseno L, Tay Y, Kats L, Pandolfi PP. A ceRNA hypothesis: the Rosetta Stone of a hidden RNA. language? Cell. 2011;146(3):353–8. 10.1016/j.cell.2011.07.014.
15. Meng J, Wang H, Chi R, Qiao Y, Wei J, Zhang Y, et al. The eTM–miR858–MYB62-like module regulates anthocyanin biosynthesis under low-nitrogen conditions in Malus spectabilis. New Phytol. 2023;238(6):2524–44. 10.1111/nph.18894.

16. Qin T, Zhao H, Cui P, Albesher N, Xiong L. A nucleus-localized long non-coding RNA enhances drought and salt stress tolerance. Plant Physiol. 2017;175(3):1321–36. 10.1104/pp.17.00574.
17. Zhang X, Shen J, Xu Q, Dong J, Song L, Wang W, et al. Long noncoding RNA lncRNA354 functions as a competing endogenous RNA of miR160b to regulate ARF genes in response to salt stress in upland cotton. Plant Cell Environ. 2021;44(10):3302–21. 10.1111/pce.14133.
18. Li B, Feng C, Zhang W, Sun S, Yue D, Zhang X, et al. Comprehensive non-coding RNA analysis reveals specific lncRNA/circRNA–miRNA–mRNA regulatory networks in the cotton response to drought stress. Int J Biol Macromol. 2023;253:126558. 10.1016/j.ijbiomac.2023.126558.
19. Zhang K, Wang W, Li J, Liang Z, Li M. Genome-wide analysis of long noncoding RNAs in response to drought stress in the seeds of Brassica napus. BMC Genomics. 2026;27(1):137. 10.1186/s12864-025-12496-8.
20. Leng Y, Sun J, Wang J, Liu H, Zheng H, Zhang M, et al. Genome-wide lncRNAs identification and association analysis for cold-responsive genes at the booting stage in rice (Oryza sativa L). Plant Genome. 2020;13(2):e20020. 10.1002/tpg2.20020.
21. Yang X, Liu C, Niu X, Wang L, Li L, Yuan Q, et al. Research on lncRNA related to drought resistance of Shanlan upland rice. BMC Genomics. 2022;23(1):336. 10.1186/s12864-022-08546-0.
22. Ye X, Wang S, Zhao X, Gao N, Wang Y, Yang Y, et al. Role of lncRNAs in cis- and trans-regulatory responses to salt in Populus trichocarpa. Plant J. 2022;110(4):978–93. 10.1111/tpj.15714.
23. Cheng B, Pei W, Wan K, Pan R, Zhang W. LncRNA cis- and trans-regulation provides new insight into drought stress responses in wild barley. Physiol Plant. 2024;176(4):e14424. 10.1111/ppl.14424.
24. Negi P, Mishra S, Ganapathi TR, Srivastava AK. Regulatory short RNAs: a decade's tale for manipulating salt tolerance in plants. Physiol Plant. 2021;173(4):1535–55. 10.1111/ppl.13492.
25. Chen X, Chen Z, Watts R, Luo H. Non-coding RNAs in plant stress responses: molecular insights and agricultural applications. Plant Biotechnol J. 2025;23(8):3195–233. 10.1111/pbi.70134.
26. Guo Y, Guo D, Wang Y, Yin J, Liu G, Xu H. Advances of long non-coding RNA in perennial plants: development and stress responses. Plants. 2025;14(21):3280. 10.3390/plants14213280.
27. Ren J, Jiang C, Zhang H, Shi X, Ai X, Li R, et al. LncRNA-mediated ceRNA networks provide novel potential biomarkers for peanut drought tolerance. Physiol Plant. 2022;174(1):e13610. 10.1111/ppl.13610.
28. Badouin H, Gouzy J, Grassa CJ, Murat F, Staton SE, Cottret L, et al. The sunflower genome provides insights into oil metabolism, flowering and Asterid evolution. Nature. 2017;546(7656):148–52. 10.1038/nature22380.
29. Liu X, Baird WV. Differential expression of genes regulated in response to drought or salinity stress in sunflower. Crop Sci. 2003;43(2):678–87. 10.2135/cropsci2003.6780.
30. Liang C, Wang W, Ma J, Wang J, Zhou F, Li W, et al. Identification of differentially expressed microRNAs of sunflower seedlings under drought stress. Agron J. 2020;112(4):2472–84. 10.1002/agj2.20254.

31. Shi H, Hou J, Li D, Hu H, Wang Y, Wu Y, et al. Comparative transcriptome and coexpression network analysis reveals key pathways and hub candidate genes associated with sunflower (Helianthus annuus L.) drought tolerance. BMC Plant Biol. 2024;24(1):224. 10.1186/s12870-024-04932-w.
32. Flórez-Zapata NMV, Reyes-Valdés MH, Martínez O. Long non-coding RNAs are major contributors to transcriptome changes in sunflower meiocytes with different recombination rates. BMC Genomics. 2016;17(1):490. 10.1186/s12864-016-2776-1.
33. Yu S, Zhang Z, Li J, Zhu Y, Yin Y, Zhang X, et al. Genome-wide identification and characterization of lncRNAs in sunflower endosperm. BMC Plant Biol. 2022;22(1):494. 10.1186/s12870-022-03882-5.
34. Liu Y, Zhou F, Huang X, Wang W, Zhang S, Feng F. Identification and integrated analysis of mRNAs, lncRNAs, and microRNAs of developing seeds in high oleic acid sunflower (Helianthus annuus L). Acta Physiol Plant. 2021;43(6):85. 10.1007/s11738-021-03259-5.
35. Fass MI, Rivarola M, Ehrenbolger GF, Maringolo CA, Montecchia JF, Quiroz F, et al. Exploring sunflower responses to Sclerotinia head rot at early stages of infection using RNA-seq analysis. Sci Rep. 2020;10(1):13347. 10.1038/s41598-020-70315-4.
36. Szcześniak MW, Wanowska E. CANTATAdb 3.0: an updated repository of plant long non-coding RNAs. Plant Cell Physiol. 2024;65(9):1486–93. 10.1093/pcp/pcae081.
37. Çelik Altunoğlu Y, Ünel NM, Baloğlu MC, Ulu F, Can TH, Çetinkaya R. Comparative identification and evolutionary relationship of fatty acid desaturase (FAD) genes in some oil crops: the sunflower model for evaluation of gene expression pattern under drought stress. Biotechnol Biotechnol Equip. 2018;32(4):846–57. 10.1080/13102818.2018.1480421.
38. Ceylan Y, Çelik Altunoğlu Y, Horuz E. HSF and Hsp gene families in sunflower: a comprehensive genome-wide determination survey and expression patterns under abiotic stress conditions. Protoplasma. 2023;260(6):1473–91. 10.1007/s00709-023-01862-6.
39. Sarel D, Büyük İ. The YABBY gene network in sunflower: evolutionary dynamics and drought-responsive expression profiling. Helia. 2025;48(83):135–53. 10.29329/helia.2025.1411.6.
40. Okay A, Kırlıoğlu T, Durdu YŞ, Akdeniz SŞ, Büyük İ, Aras ES. Omics approaches to understand the MADS-box gene family in common bean (Phaseolus vulgaris L.) against drought stress. Protoplasma. 2024;261(4):709–24. 10.1007/s00709-024-01928-z.
41. Chen S, Zhou Y, Chen Y, Gu J. fastp: an ultra-fast all-in-one FASTQ preprocessor. Bioinformatics. 2018;34(17):i884–90. 10.1093/bioinformatics/bty560.
42. Kim D, Paggi JM, Park C, Bennett C, Salzberg SL. Graph-based genome alignment and genotyping with HISAT2 and HISAT-genotype. Nat Biotechnol. 2019;37(8):907–15. 10.1038/s41587-019-0201-4.
43. Wang L, Wang S, Li W. RSeQC: quality control of RNA-seq experiments. Bioinformatics. 2012;28(16):2184–5. 10.1093/bioinformatics/bts356.
44. Pertea M, Pertea GM, Antonescu CM, Chang TC, Mendell JT, Salzberg SL. StringTie enables improved reconstruction of a transcriptome from RNA-seq reads. Nat Biotechnol. 2015;33(3):290–5. 10.1038/nbt.3122.

45. Pertea G, Pertea M. GFF utilities: GffRead and GffCompare. F1000Research. 2020;9:304. 10.12688/f1000research.23297.2.
46. Wucher V, Legeai F, Hédan B, Rizk G, Lagoutte L, Leeb T, et al. FEELnc: a tool for long non-coding RNA annotation and its application to the dog transcriptome. Nucleic Acids Res. 2017;45(8):e57. 10.1093/nar/gkw1306.
47. Tian XC, Nie S, Domingues D, Rossi Paschoal A, Jiang LB, Mao JF. PlantLncBoost: key features for plant lncRNA identification and significant improvement in accuracy and generalization. New Phytol. 2025;247(3):1538–49. 10.1111/nph.70211.
48. Kang YJ, Yang DC, Kong L, Hou M, Meng YQ, Wei L, et al. CPC2: a fast and accurate coding potential calculator based on sequence intrinsic features. Nucleic Acids Res. 2017;45(W1):W12–6. 10.1093/nar/gkx428.
49. Mistry J, Chuguransky S, Williams L, Qureshi M, Salazar GA, Sonnhammer ELL, et al. Pfam: the protein families database in 2021. Nucleic Acids Res. 2021;49(D1):D412–9. 10.1093/nar/gkaa913.
50. Eddy SR. Accelerated profile HMM searches. PLoS Comput Biol. 2011;7(10):e1002195. 10.1371/journal.pcbi.1002195.
51. Nawrocki EP, Eddy SR. Infernal 1.1: 100-fold faster RNA homology searches. Bioinformatics. 2013;29(22):2933–5. 10.1093/bioinformatics/btt509.
52. Kalvari I, Nawrocki EP, Ontiveros-Palacios N, Argasinska J, Lamkiewicz K, Marz M, et al. Rfam 14: expanded coverage of metagenomic, viral and microRNA families. Nucleic Acids Res. 2021;49(D1):D192–200. 10.1093/nar/gkaa1047.
53. Love MI, Huber W, Anders S. Moderated estimation of fold change and dispersion for RNA-seq data with DESeq2. Genome Biol. 2014;15(12):550. 10.1186/s13059-014-0550-8.
54. Langfelder P, Horvath S. WGCNA: an R package for weighted correlation network analysis. BMC Bioinformatics. 2008;9(1):559. 10.1186/1471-2105-9-559.
55. Dai X, Zhuang Z, Zhao PX. psRNATarget: a plant small RNA target analysis server (2017 release). Nucleic Acids Res. 2018;46(W1):W49–54. 10.1093/nar/gky316.
56. Shannon P, Markiel A, Ozier O, Baliga NS, Wang JT, Ramage D, et al. Cytoscape: a software environment for integrated models of biomolecular interaction networks. Genome Res. 2003;13(11):2498–504. 10.1101/gr.1239303.
57. Cantalapiedra CP, Hernández-Plaza A, Letunic I, Bork P, Huerta-Cepas J. eggNOG-mapper v2: functional annotation, orthology assignments, and domain prediction at the metagenomic scale. Mol Biol Evol. 2021;38(12):5825–9. 10.1093/molbev/msab293.
58. Huerta-Cepas J, Szklarczyk D, Heller D, Hernández-Plaza A, Forslund SK, Cook H, et al. eggNOG 5.0: a hierarchical, functionally and phylogenetically annotated orthology resource. Nucleic Acids Res. 2019;47(D1):D309–14. 10.1093/nar/gky1085.
59. Bustin SA, Benes V, Garson JA, Hellemans J, Huggett J, Kubista M, et al. The MIQE guidelines: minimum information for publication of quantitative real-time PCR experiments. Clin Chem. 2009;55(4):611–22. 10.1373/clinchem.2008.112797.

60. Livak KJ, Schmittgen TD. Analysis of relative gene expression data using real-time quantitative PCR and the 2 − ΔΔCT method. Methods. 2001;25(4):402–8. 10.1006/meth.2001.1262.

61. Sarel D, Yerli N, Büyük İ. Long non-coding RNA landscape and ceRNA networks underlying the drought response of Cannabis sativa L. BMC Plant Biol. 2026. 10.1186/s12870-026-09380-2.

Figures

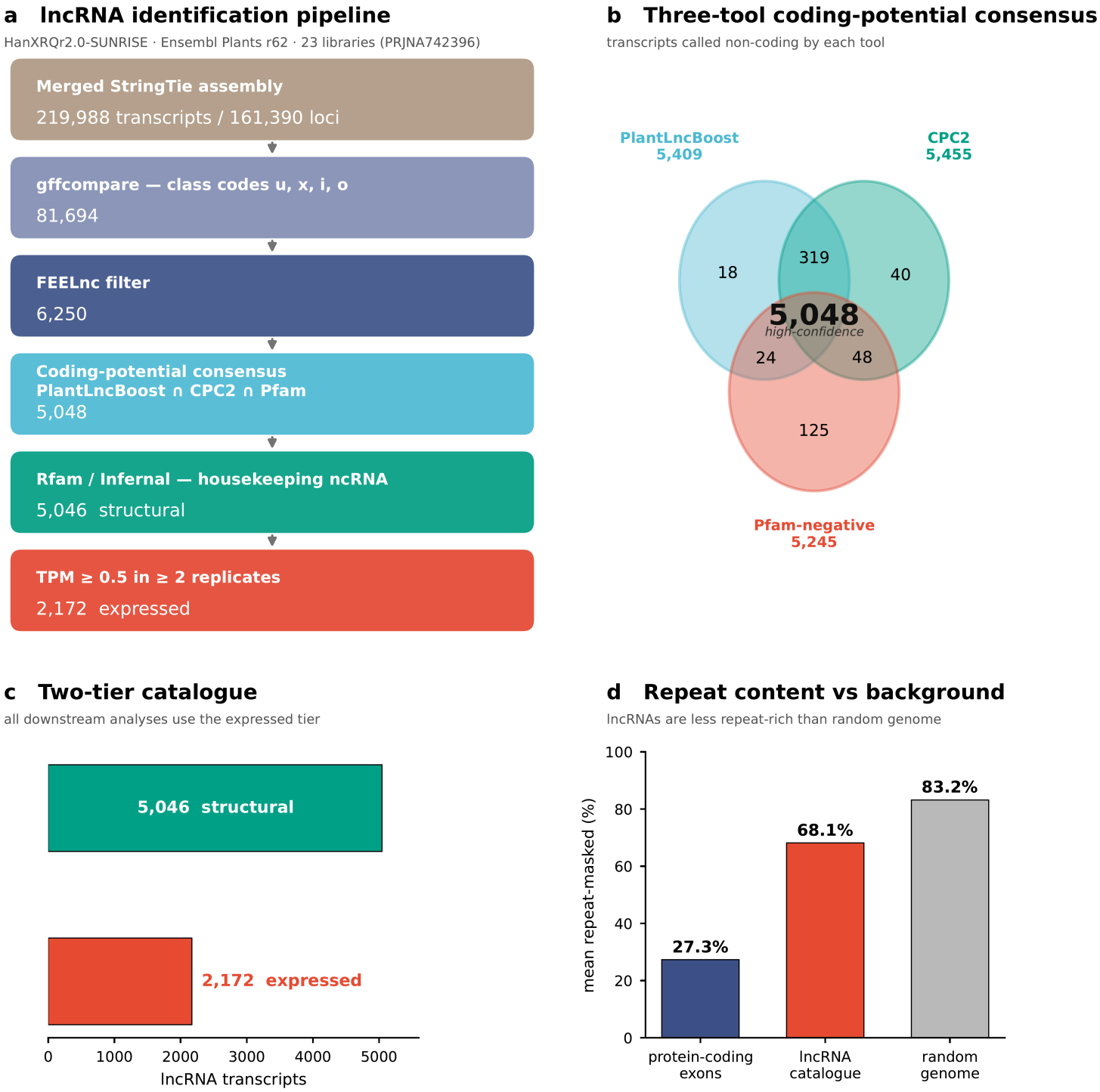


Figure 1

Genome-wide identification of *Helianthus annuus* long non-coding RNAs (lncRNAs) and the two-tier catalogue. (a) Identification pipeline as a funnel: 219,988 assembled transcripts (161,390 loci) → gffcompare strict class codes u/x/i/o → 81,694 novel candidates → FEELnc_filter (≥ 200 nt; sense-exon overlap removed; mono-exonic discarded) → 6,250 → three-tool plant-aware coding-potential consensus (PlantLncBoost, CPC2, Pfam-negative) → 5,048 high-confidence lncRNAs → Rfam/Infernal removes 2 housekeeping ribosomal RNAs (rRNAs) → 5,046 structurally validated → expression floor (TPM [transcripts per million] ≥ 0.5 in ≥ 2 biological replicates of ≥ 1 stress×tissue group) → 2,172 expressed. (b) Three-way Venn of the coding-potential tools: only-PlantLncBoost 18, only-CPC2 40, only-Pfam 125, PlantLncBoost∩CPC2 319, PlantLncBoost∩Pfam 24, CPC2∩Pfam 48, all-three unanimous non-coding 5,048. (c) Two-tier catalogue schematic: 5,046 structurally validated versus 2,172 expressed lncRNAs; the expressed tier underpins all downstream analyses. (d) Repeat-content quality control: mean repeat-masked content of lncRNA exons 68.1%, protein-coding exons 27.3%, and length-matched random genomic intervals 83.2%. The catalogue was assembled from the 23 usable libraries of PRJNA742396; the differential-expression analyses in Fig. 2 rest on the 21 that remained after two principal-component outliers were removed (Methods).

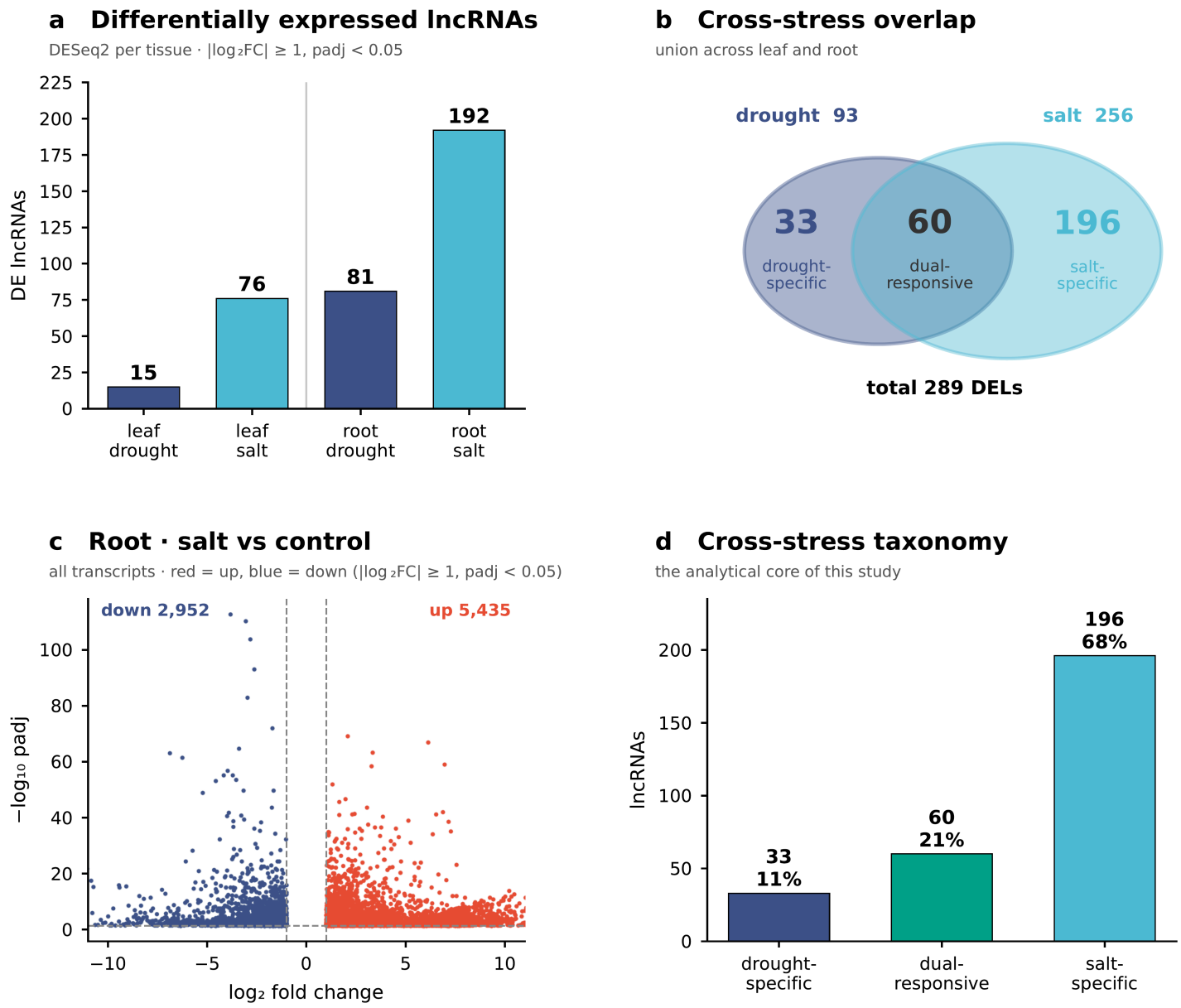


Figure 2

Drought- and salt-responsive long non-coding RNAs (lncRNAs) and the response taxonomy. Differential expression called by DESeq2 per tissue (|log2FC| ≥ 1 & padj < 0.05), contrasts drought-vs-control and salt-vs-control (stresses applied and tested separately). (a) Differentially expressed lncRNA (DEL) counts per contrast: leaf-drought 15, leaf-salt 76, root-drought 81, root-salt 192 (bar chart). (b) Two-set Venn overlap of drought-responsive (93) and salt-responsive (256) DELs, partitioning the 289 unique DELs into drought-specific 33, dual-responsive 60 (significant in both single-stress contrasts) and salt-specific 196 (Venn set colours). (c) Volcano plot of transcriptome-wide differential expression in root under salinity, the contrast with the largest response: 2,952 down- and 5,435 up-regulated transcripts; x-axis log2FC, y-axis −log10(padj), points coloured by regulation direction, dashed significance thresholds. (d) The 289 DELs by response class (bar chart): drought-specific 33 (11%), dual-responsive 60 (21%), salt-specific 196 (68%).

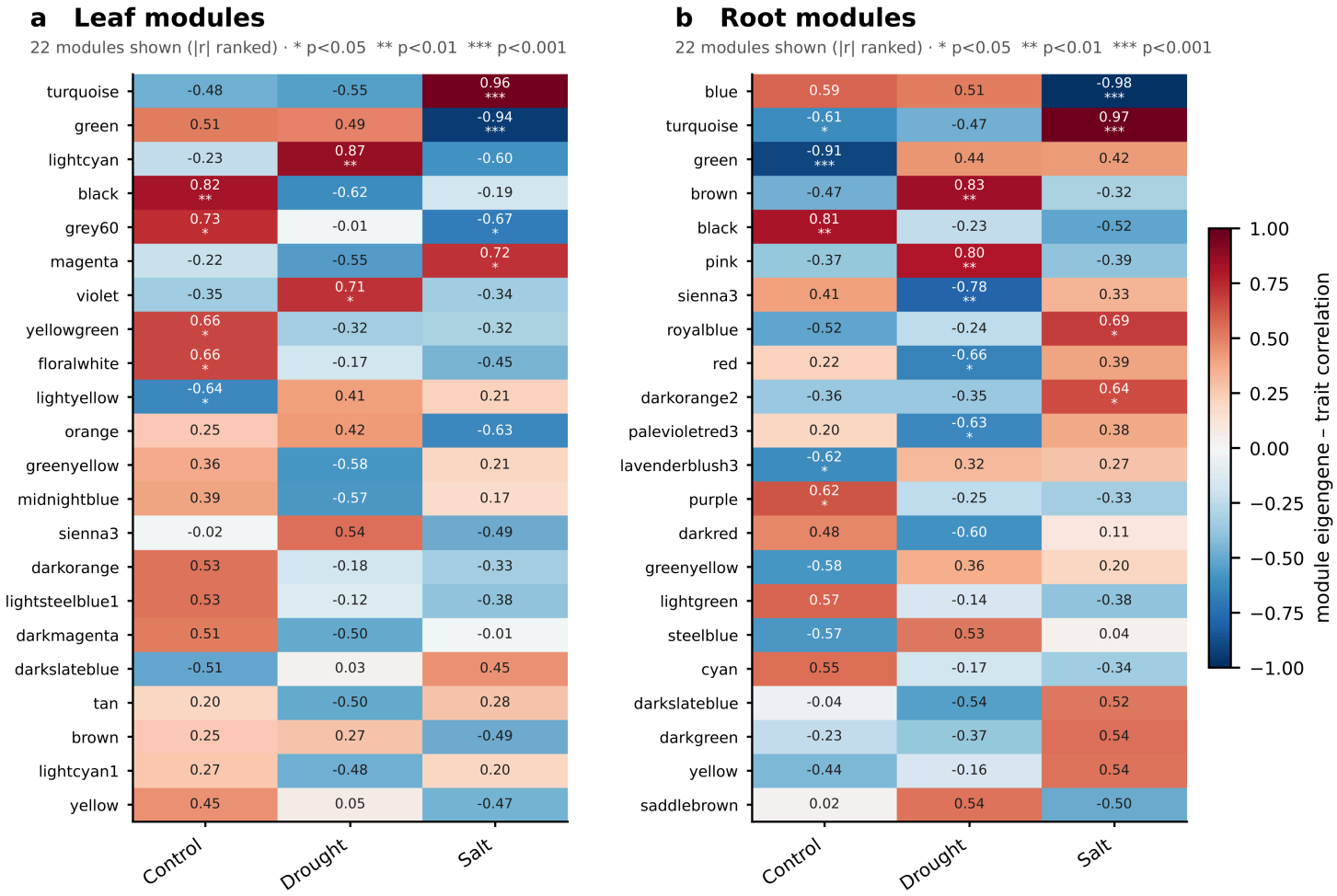


Figure 3

Stress-associated co-expression modules from per-tissue weighted gene co-expression network analysis (WGCNA). Signed networks constructed separately for leaf and root; heatmaps show module eigengene (ME)–trait correlations (salient modules |r| > 0.5, p < 0.05). In each panel the 22 modules with the largest |r| are shown. (a) Leaf network (soft-thresholding power β = 5; scale-free R^2 = 0.872; 50 modules in total), highlighting turquoise (salt r = 0.96, p < 0.001), green (salt r = −0.94, p < 0.001) and lightcyan (drought r = 0.87, p < 0.01). (b) Root network (β = 4; R^2 = 0.905; 59 modules in total): turquoise (salt r = 0.97, p < 0.001), blue (salt r = −0.98, p < 0.001), brown (drought r = 0.83, p < 0.01) and pink (drought r = 0.80, p < 0.01). Drought and salinity, tested separately, track distinct modules per tissue. Cell colour encodes correlation sign/magnitude; r (p) annotated.

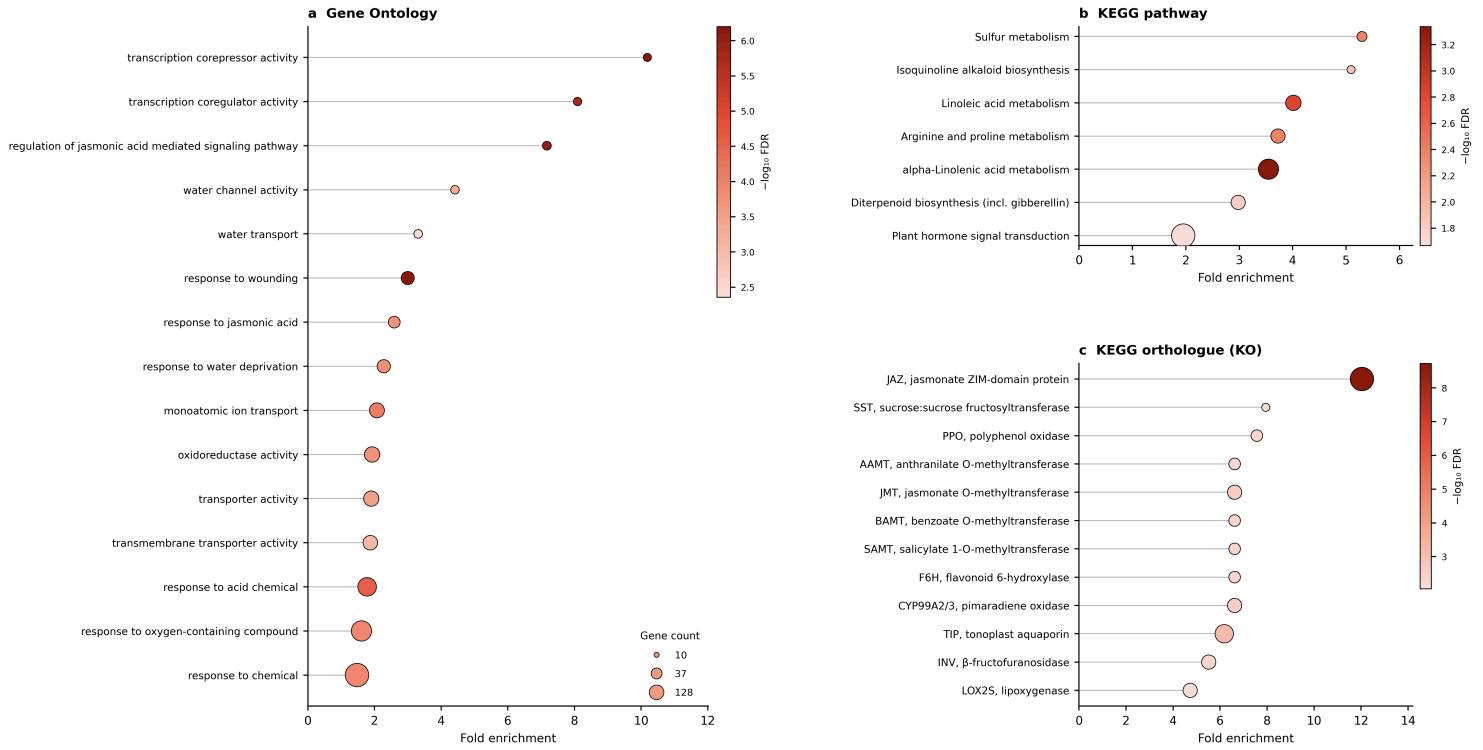


Figure 4

Predicted differentially expressed long non-coding RNA (DEL)-anchored lncRNA–miRNA–mRNA competing-endogenous-RNA (ceRNA) network under drought and salinity (tested separately). Construction (predicted, sequence-based): 892 miRNAs (microRNAs; han-/ath-/gma-, miRBase) screened by psRNATarget (Expectation ≤ 5) against 289 DELs and 694 module-associated differentially expressed gene (DEG) mRNAs (messenger RNAs); an edge denotes ≥ 1 shared miRNA AND co-membership of the same non-grey WGCNA (weighted gene co-expression network analysis) module. Full network: 2,575 lncRNA–mRNA edges, 1,041 nodes (111 lncRNAs, 540 mRNAs, 390 miRNAs), 3,278 lncRNA–miRNA–mRNA triplets. (a) Core sub-network — edges with ≥ 3 shared miRNAs OR involving a qRT-PCR (quantitative reverse-transcription PCR)-panel lncRNA: 254 edges, 44 lncRNAs, 176 mRNAs; nodes coloured by molecule type, edge width scaled to shared-miRNA count. (b) Dual-responsive exemplar: MSTRG.59498.1 (a DEL significant in both the drought and salt single-stress contrasts) linked via 4 miRNAs (ath-miR4243, ath-miR837-5p, ath-miR866-5p, gma-miR1512a-3p) to 22 mRNAs across 23 triplets.

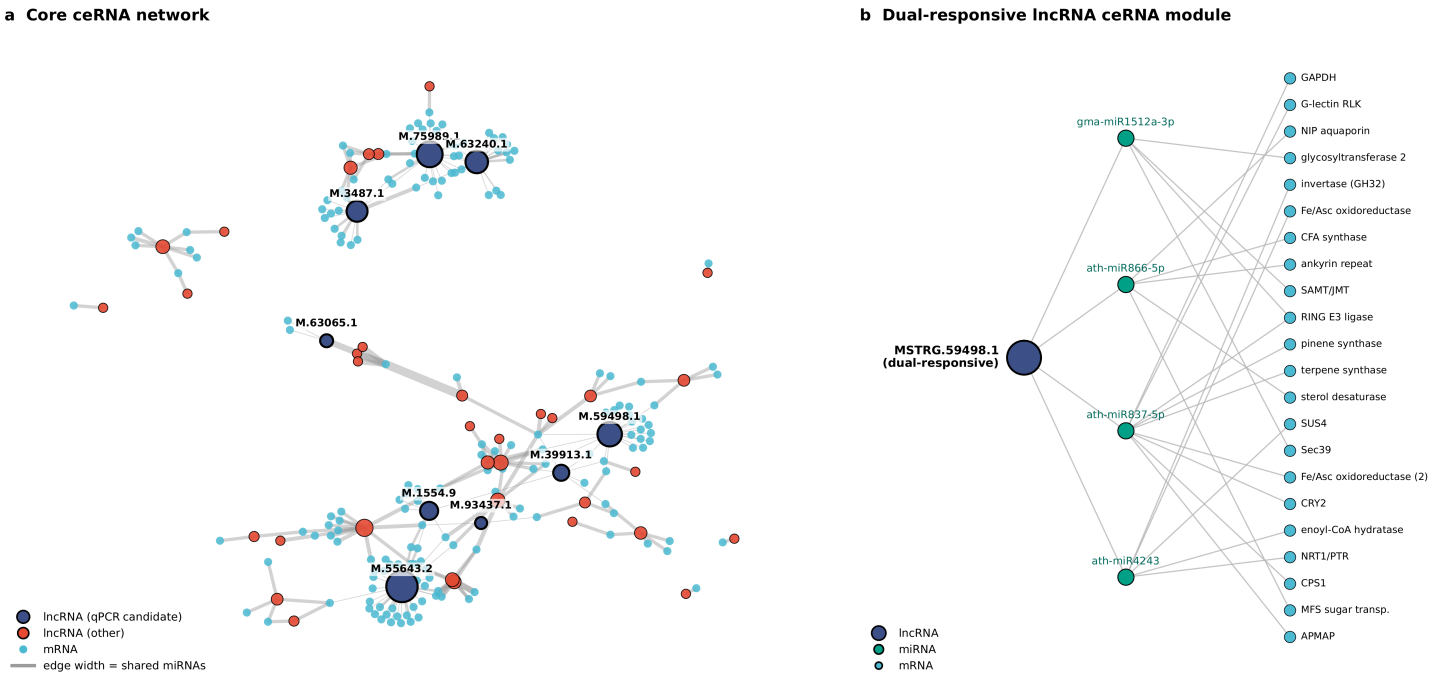


Figure 5

Functional over-representation of the predicted competing-endogenous-RNA (ceRNA) network mRNA layer. Hypergeometric over-representation test (Benjamini–Hochberg false discovery rate, BH-FDR < 0.05) on the 540 network mRNAs (521 annotated by eggNOG-mapper v2; background 6,900 annotated differentially expressed genes), yielding a reportable significant set of 115 Gene Ontology (GO) terms, 7 KEGG pathways and 15 KEGG-Orthology (KO) terms. All three panels are dotplots: x-axis fold enrichment, dot size network-mRNA count, colour BH-FDR. (a) GO over-representation, showing the 15 terms with the lowest BH-FDR of the 115 reportable. (b) KEGG pathways, all 7 reportable. (c) KEGG-Orthology, showing the 12 terms with the lowest BH-FDR of the 15 reportable. Two convergent themes highlighted. Jasmonate signalling/biosynthesis: regulation of jasmonate-mediated signalling (GO:2000022, 7.1-fold), transcription-corepressor activity (GO:0003714, 10.0-fold; in keeping with the jasmonate-ZIM-domain (JAZ) corepressor role), JAZ repressor (K13464), α-linolenic acid metabolism (map00592), lipoxygenase. Water/ion homeostasis: water-channel activity (GO:0015250, 4.4-fold, BH-FDR 4.3e-4), response to water deprivation (GO:0009414, 2.3-fold), tonoplast intrinsic protein (TIP) aquaporin (K09873), monoatomic ion transport (GO:0006811), abscisic-acid-linked protein phosphatase 2C (K14497), plant hormone signal transduction (map04075).

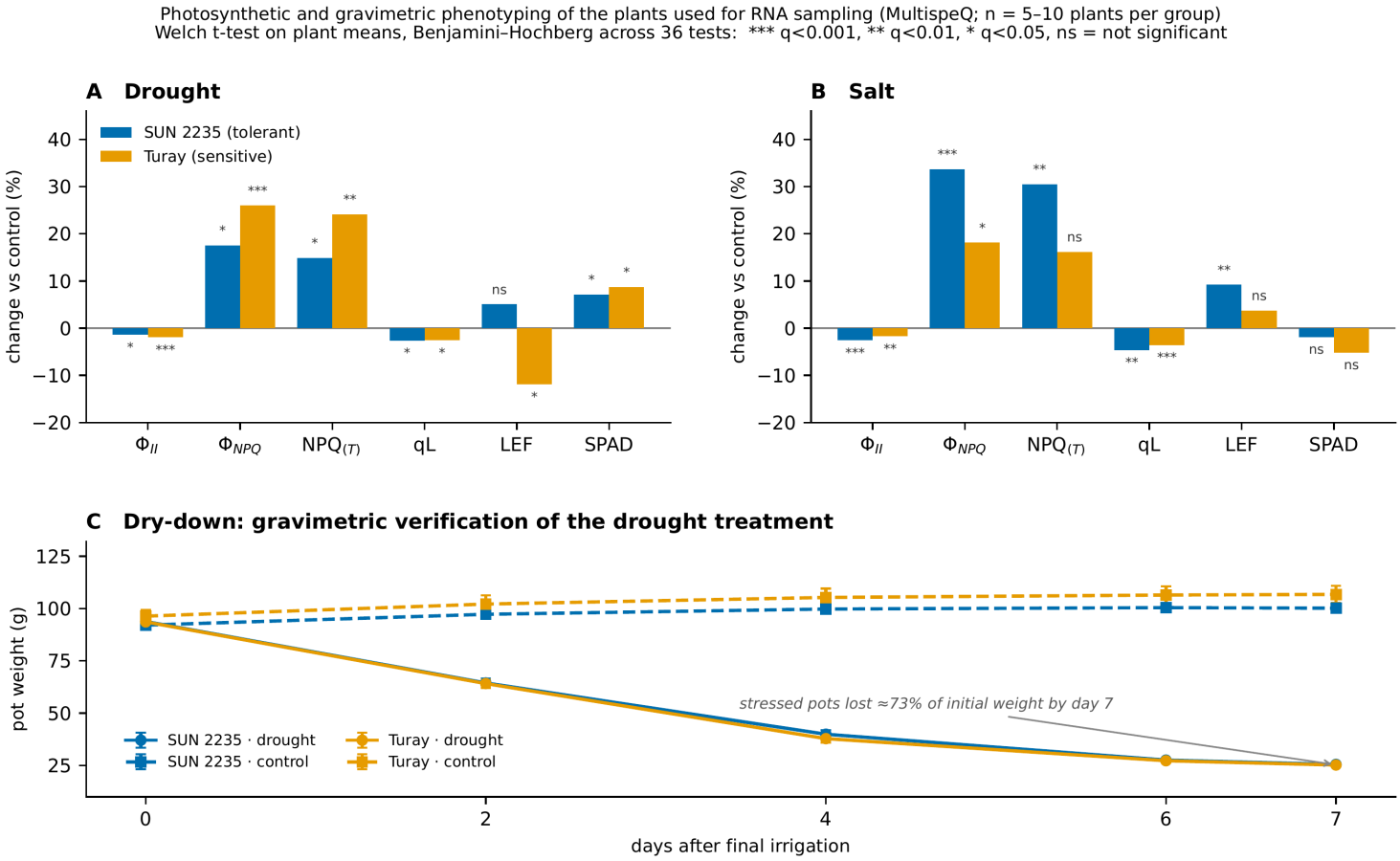


Figure 6

Photosynthetic and gravimetric phenotyping of the treated plant cohort from which RNA was sampled, in a drought-tolerant and a drought-sensitive sunflower (*Helianthus annuus*) cultivar under drought and salinity. Chlorophyll-fluorescence parameters were recorded with a MultispeQ v2 handheld fluorometer (PhotosynQ) on light-adapted leaves of the treated cohort from which the RNA-sampled plants were drawn; three leaves were averaged per plant, making the plant the unit of analysis (drought: cv. SUN 2235 n = 5 control / 9 stress, cv. Turay n = 5 / 10; salinity: n = 7 per group). (A, B) Percent change relative to the matched within-cultivar control for the quantum yield of photosystem II (Φ_II), the quantum yield of regulated non-photochemical dissipation (Φ_NPQ), non-photochemical quenching NPQ(T), the fraction of open photosystem II centres (qL), linear electron flow (LEF) and relative chlorophyll content (SPAD), under drought (A) and salinity (B), for the drought-tolerant cv. SUN 2235 (blue) and the drought-sensitive cv. Turay (orange). Significance is from Welch's unequal-variance *t*-tests of stress against matched control within cultivar, Benjamini–Hochberg-corrected across all 36 tests, of which 26 reached $q < 0.05$ (* $q < 0.05$, ** $q < 0.01$, *** $q < 0.001$, ns = not significant). Panels A and B show six of the nine parameters recorded; the quantum yield of non-regulated dissipation (Φ_NO), Fv'/Fm' and leaf temperature are not plotted, and the leaf-temperature contrast is reported in the Results. No cultivar × treatment interaction model was fitted, so between-cultivar statements are descriptive contrasts of within-cultivar responses. (C) Gravimetric verification of the drought treatment: pot weight (mean ± standard error) on days 0, 2, 4, 6 and 7 after final irrigation for all four drought groups. Droughted pots lost 72.8% (SUN 2235, n = 9) and

73.1% (Turay, *n* = 10) of their initial weight while control pots gained 8.8% and 10.7% (*n* = 5 each), the two cultivars drying at indistinguishable rates. These are single-time-point, light-adapted fluorescence measurements: gas exchange, water potential and tissue ion content were not measured, and the data characterize the physiological state of the sampled plants rather than testing the predicted competing-endogenous-RNA network.

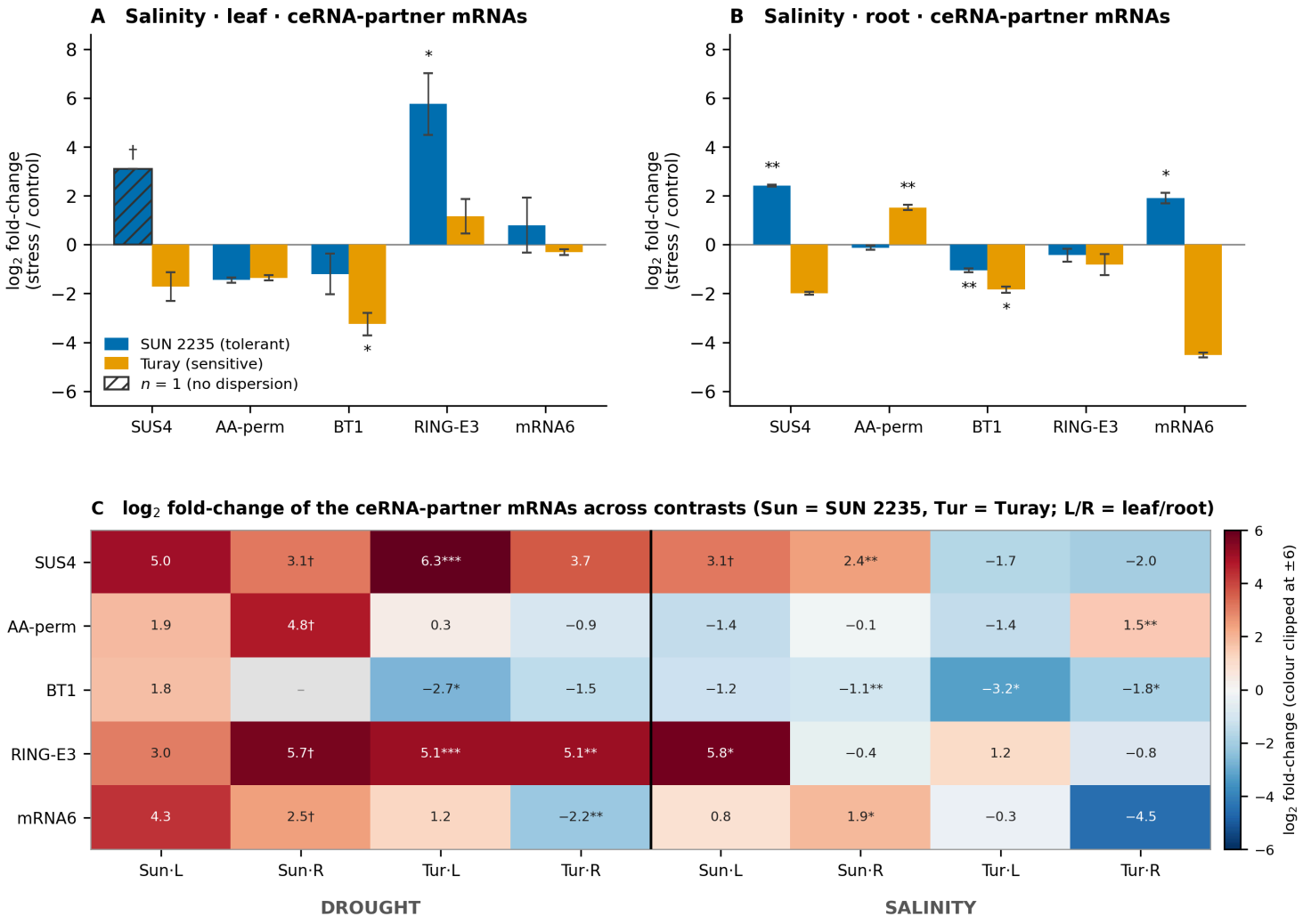


Figure 7

Expression of the predicted competing-endogenous-RNA (ceRNA) network partner messenger RNAs (mRNAs) by qRT-PCR in a drought-tolerant and a drought-sensitive sunflower (*Helianthus annuus*) cultivar. Relative expression was measured by the 2^−ΔΔCT method with normalization to the geometric mean of ACTIN and elongation factor 1-α, each stress being expressed against its own matched control (same stress, cultivar and tissue). The five partner mRNAs are sucrose synthase SUS4, an amino-acid permease (AA-perm), BT1, a RING-type E3 ligase (RING-E3) and HanXRQr2_Chr07g0278911 (mRNA6). (A, B) $\log_2$ fold-change under salinity in leaf (A) and root (B) for the drought-tolerant cv. SUN 2235 (blue) and the drought-sensitive cv. Turay (orange); bars show the mean of the stress group with its standard error. (C) $\log_2$ fold-change across the eight stress × cultivar × tissue contrasts (Sun, cv. SUN 2235; Tur, cv. Turay; L, leaf; R, root); printed values are unclipped, the colour scale saturates at ±6, and grey cells

denote contrasts not determined. In all panels, asterisks denote exploratory, uncorrected Welch *t*-tests (* $p < 0.05$, ** $p < 0.01$, *** $p < 0.001$); of the 34 computable partner-mRNA contrasts, 12 were nominally significant and 7 remained so after Benjamini–Hochberg correction ($q < 0.05$). † marks single-replicate contrasts, drawn as hatched bars in A, which carry no dispersion. The co-measured long non-coding RNA assays did not meet the specificity and detection criteria and are not shown (Additional file 1).

Supplementary Files

This is a list of supplementary files associated with this preprint. Click to download.

- Additionalfile1.docx
- Additionalfile2.xlsx
- FigureS1.png